JOURNAL OF MATERIALS SCIENCE 17 (1982) 1337–1347

Structural investigation of boron-containing metallic glasses

H. S. CHEN
Bell Laboratories, Murray Hill, New Jersey 07974, USA

T. FUJIWARA
Institute of Materials Science, University of Tsukuba, Ibaraki 305, Japan

Y. WASEDA
The Research Institute of Mineral Dressing and Metallurgy, (SENKEN), Tohuku University, Sendai 980, Japan

Structural investigations have been made of high boron-containing alloy glasses of compositions $Co_{100-x}B_x$ with $x = 34$, 36, 38 and 40 at % measured by X-ray diffraction. The characteristic second-peak splitting in the radial distribution function (RDF) is found for all samples presently investigated. The shoulders are also observed near the distances of 0.20 and 0.34 nm. The partial radial distribution functions of Co–Co and Co–B pairs have been derived from the measured total RDF data by applying the concentration method with the anomalous scattering technique, and the contributions from different atomic pairs to total RDF have been discussed. The calculation by the relaxed dense random packing model has been made for Fe–B alloy glasses with three different boron concentrations, i.e., 15, 25, and 40 at % boron and a comparison between the calculated and experimentally determined data is presented. The present model calculation could give the possible representation for the compositional dependence of the X-ray RDF for amorphous Fe–B alloys with boron contents of up to 40 at % as well as the different peak profile observed in the total RDF of X-ray data between Fe–B and Fe–P glasses.

1. Introduction

There has been a great deal of attention devoted to the atomic scale structure and many physical and chemical properties of various metallic glasses produced by rapid quenching from the melt. In particular, the current interest in this field focuses on the Fe–B base alloys because of their excellent features, such as their large saturation magnetizations and Invar characteristics (see, for example [1]). In the Fe–B base alloy glasses, a break in compositional dependence at 18 at% B content has been found in the measurements of density [2], activation energy of crystallization [3] and saturation magnetic moment [4]. In this respect, one can expect that the changes of the structure by the boron content should not be monotonic. In fact, X-ray diffraction data indicate the compositional dependence of the ratio of the sub-peak heights of split second peak in the radial distribution function (RDF) [5].

The structural feature, i.e., the second sub-peak being more intense than the first sub-peak in the X-ray RDF for glasses with the boron content less than 18 at%, differs from that of other typical metal–metalloid-type glasses, such as the Fe–P and Pd–Si systems containing 15 to 25 at% metalloids. However, with increasing boron contents, the first sub-peak becomes more intense at the expense of the second one, and the peak profile rather resembles that observed for most metal–metalloid glasses. The characteristic feature in the X-ray RDF for the glass containing less than

0022–2461/82/051337–11$03.82/0

18 at% boron seems to contradict the total RDF of $Fe_{23}B_{17}$, recently obtained from neutron diffraction experiments [6]. However, this apparent discrepancy arises mainly from the large contribution of the Fe–B pairs to the total RDF in the neutron diffraction data and the Fe–Fe partial RDF is found to be very close to that from the X-ray RDF [7]. In addition, the recent model calculation of amorphous $Fe_{85}P_{15}$ [8] and $Fe_{85}B_{15}$ [7] suggested that the relaxed dense random packing (DRP) model gives a good reproduction of the characteristic peak profile of the X-ray RDF for both alloy glasses. These results prompted us to carry out further investigation on the structure of metallic glasses containing higher boron concentrations.

This paper reports the structural models for three different boron concentrations, i.e., 15, 25 and 40 at% boron and experimental RDF for corresponding alloy glasses. A comparison between the calculations and experimental data is presented, and the composition dependence of the X-ray RDF and its implications are discussed.

2. Model construction

The model structure was constructed by the two-step procedure consisting of a random packing of constituent atoms of two different sizes and structural relaxation by appropriate pair potentials. They were very similar to those described in detail in the previous work for the Fe–P system [8] and, consequently, only minor modifications used in this work are given below.

The diameter of boron atoms is set to be 0.58σ, where σ is the diameter of iron atoms. The diameter ratio is determined from the position of the Fe–B potential minimum which is calculated from the Fe–Fe and B–B potential with an appropriate averaging procedure [8]. For the homogenity of the model systems, the limiting inter-atomic distances of non-existence of the B–B pairs have to be reduced with the boron content, x, and 1.3σ, 1.2σ, and 0.9σ for $x = 15$, $x = 25$ and $x = 40$, in at%, respectively. The system size is 1500 spheres with free boundary condition. After a 100 cycle iteration procedure of the structural relaxation, a reduction of 20% was achieved in the final potential energy and a further iteration step produced a change of 0.02% in the total energy and a change of 0.0015σ in the average displacement. Any visible change of the structure was not detected by further relaxation procedure.

3. Analysis of X-ray scattering intensity patterns

Although the glassy $Fe_{60}B_{40}$ alloy is not available at the present time, the amorphous phase formation was found in higher boron concentration up to about 40 at% for Ni- and Co-base binary alloys [9]. Since almost similar atomic sizes are expected for Fe and Co atoms, glassy samples of $Co_{100-x}B_x$ in the shape of ribbon (1.0 mm width and 0.03 mm thickness) were prepared in this work by melt-quenching using the single-roller technique. The compositions studied were $Co_{100-x}B_x$ with $x = 34, 36, 38$ and 40 at%.

The basic arrangements for the measurement and operation procedures for X-ray scattering intensity and the correction of the observed intensity data were essentially similar to those employed in the works on non-crystalline materials [5, 10]. The measurements carried out in the wave vector, Q, range between 10 and 170 nm^{-1} have been smoothly extrapolated to zero at $Q = 0\,nm^{-1}$. The effect of the extrapolation and truncation up to $Q = 170\,nm^{-1}$ is known to give no critical contribution in the calculation of the RDF [10, 11]. The radial distribution function $G(r)$ is estimated in the following Fourier transformation:

$$G(r) = 4\pi r(\rho(r) - \rho_0) = \frac{2}{\pi}\int_0^\infty Q\, i(Q) \sin(Qr)\, dQ, \quad (1)$$

where $i(Q)$ is the so-called reduced interference function, $\rho(r)$ is the radial density function and ρ_0 is the average number density of atoms.

The accumulated counts varying from 7×10^4 at low angles to 2×10^5 at high angles were chosen in this work to hold counting statistics approximately uniform. The error in the structural data, $i(Q)$ and $G(r)$, obtained in this work was of the order of 1.8% following the works of Rahman [12], Greenfield *et al.* [13] and Kaplow *et al.* [14].

4. Results and discussion

4.1. Experimental information on the structure of glassy $Co_{100-x}B_x$

The reduced interference function $Q\,i(Q)$ and the radial distribution function $G(r)$ for amorphous alloys of $Co_{100-x}B_x$ with four different boron concentrations are given in Figs 1 and 2 and the relevant values such as density and peak positions are listed in Table I. The density of the samples was measured using the Archimedes' method. As shown

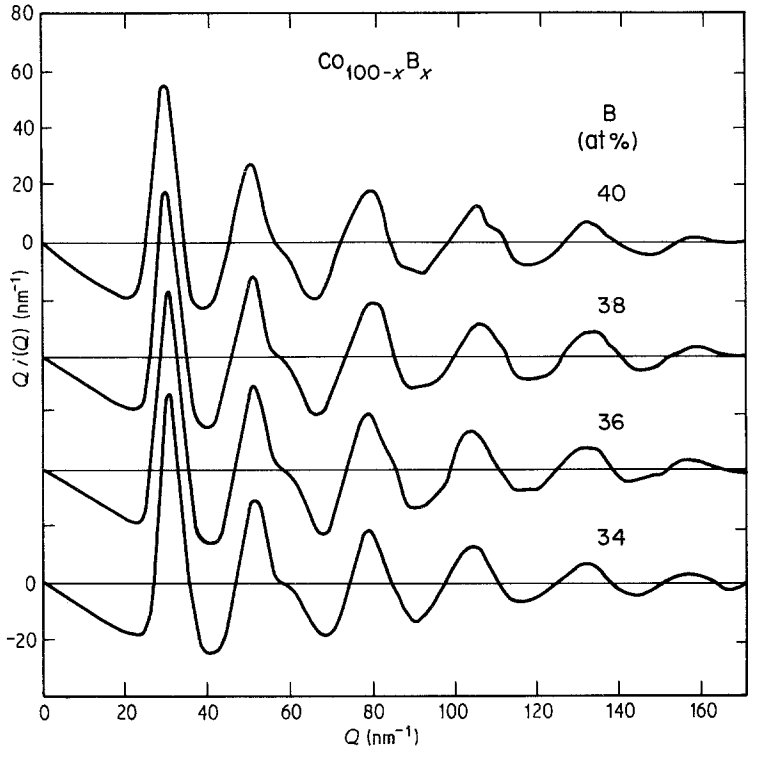

Figure 1 Function $Q\,i(Q)$ for alloy glasses of $Co_{100-x}B_x$.

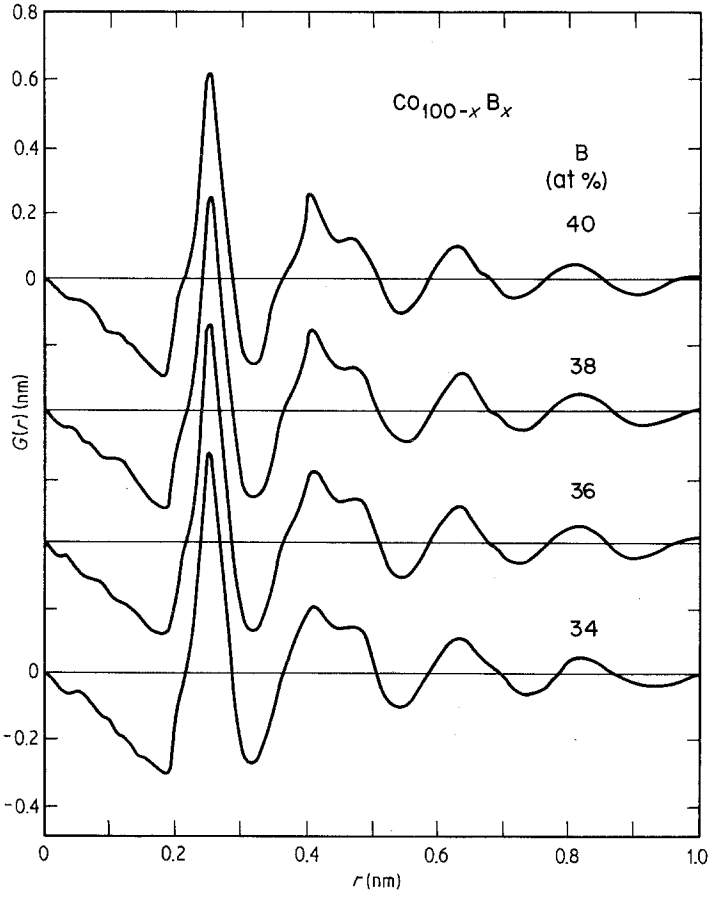

Figure 2 Function $G(r)$ for alloy glasses of $Co_{100-x}B_x$.

TABLE I Density and peak positions in alloy glasses of $Co_{100-x}B_x$

Alloy glass	Density ($g\,cm^{-3}$)	$Q\,i(Q)$ (nm^{-1})			$G(r)$ (nm)		
		1st	2nd	Shoulder	1st	2nd	(2nd)
$Co_{66}B_{34}$	7.79	29.3	52.3	60.6	0.260	0.418	0.418
$Co_{64}B_{36}$	7.67	29.4	52.3	60.6	0.259	0.418	0.480
$Co_{62}B_{38}$	7.61	29.9	52.6	60.7	0.257	0.408	0.471
$Co_{60}B_{40}$	7.48	30.1	52.7	60.8	0.257	0.406	0.463

in Figs 1 and 2, the basic profile of $Q\,i(Q)$ and $G(r)$ of boron-rich Co-base alloy glasses ($34 \leqslant x \leqslant 40$) could be classified into the same group of various metallic glasses previously investigated [10]. Namely, the profile of all the samples is composed of a relatively sharp first peak and subsequent small oscillations. We also found the second peak shoulder in $Q\,i(Q)$ and the second peak splitting in $G(r)$. The amplitude in the oscillations of both structural functions is similar to the behaviour found in typical metal–metalloid glasses, such as the Fe–P system (see Fig. 3), rather than the hypereutectic $Fe_{85}B_{15}$ alloy (see Fig. 4). It may be also noted from the experimental data for the Fe–B glasses that the recent results of $Fe_{100-x}B_x$ ($x = 14$, 15 and 17 at%) [7, 15] give a more enhanced first sub-peak in the split second-peak region of the X-ray RDF, compared with the previous results of $Fe_{84}B_{16}$ [5], i.e., the height of the first sub-peak is approximately equal to that of the second sub-peak, as shown in Fig. 4. Probably the so-called structural relaxation in metallic glasses may account for part of this difference, because the degree of structural relaxation depends upon the sample preparation and annealing conditions [10, 16], so that it is not surprising that there are small variations among metallic glass samples in the magnitude of oscillations in RDF. The noteworthy point drawn from these current experimental data is that the conclusion obtained in the previous results of $Fe_{84}B_{16}$ is still valid for the Fe–B glass with hypereutectic compositions,

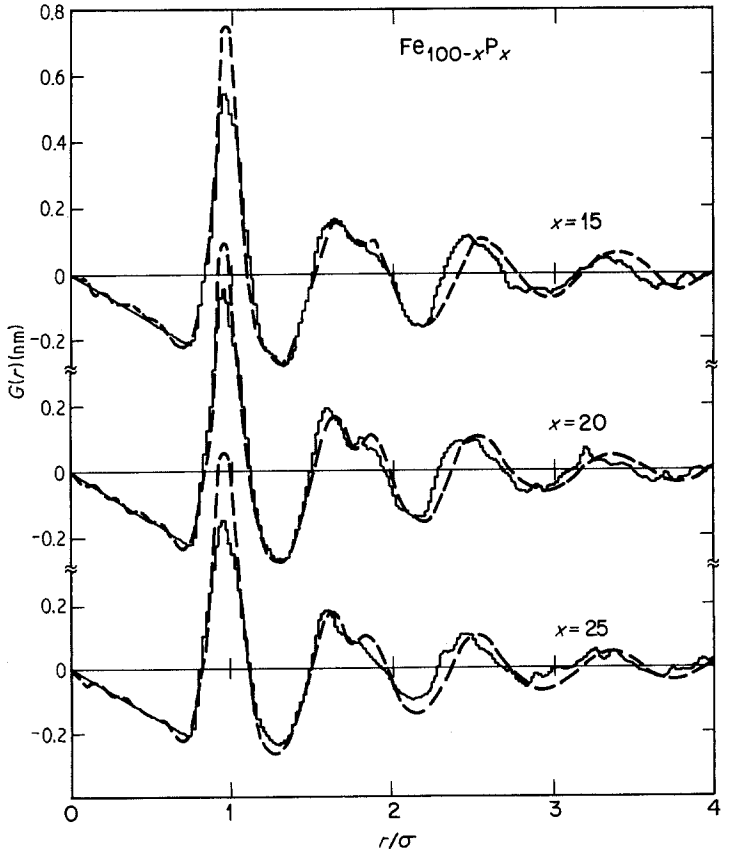

Figure 3 A comparison of model calculation with experimental data in the total RDF of $Fe_{100-x}P_x$ glasses. Histogram: relaxed DRP model; broken curve: experimental data [15].

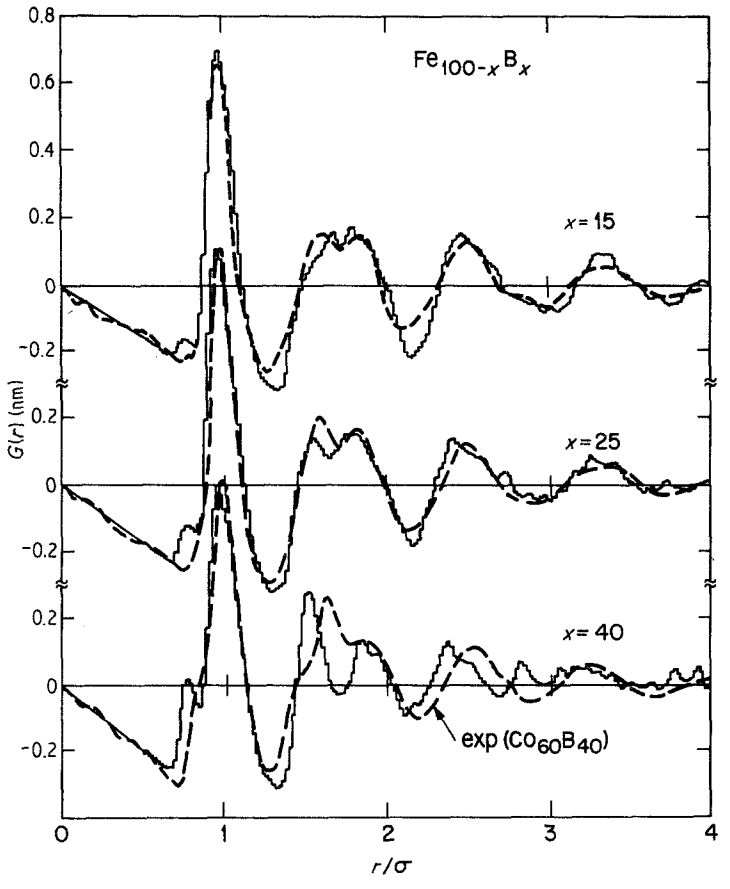

Figure 4 A comparison of model calculation with experimental data in the total RDF. Histogram: relaxed DRP model; broken curve: experimental data [7, 15].

i.e., the peak profile of the split second peak in the total RDF for the hypereutectic Fe–B glasses differs slightly from that of the typical metal–metalloid glasses. A similar structural behaviour was also found for low boron containing glass of $(W, Ru)_{80}Al_{10}B_{10}$ [17] and hypereutectic alloy liquids of $Fe_{90}B_{10}$ and $Fe_{83}B_{17}$ [18].

As shown in the results of Table I, the first peak position in $G(r)$, r_1, tends to decrease with metalloid boron contents from 0.260 nm for $x =$ 34 to 0.257 nm for $x = 40$. This is contrary to the behaviour observed for metal–metalloid glasses with $x \leqslant 25$ in which r_1 increases with x although r_1, for all samples, expands due to the addition of metalloids as compared with $r_1 \cong 0.255$ nm for the amorphous state of metal elements of M($M =$ Fe, Co and Ni). The gradual decrease observed in the glasses of higher boron contents implies a consequent exchange in the positions between metal atoms and boron atoms, because of the complete filling-up of the vacant spaces available in the dense random packing (DRP) structure formed by the metal atoms in the higher boron concentration glasses.

On the basis of the previous experimental data for various metallic glasses [10], the observed total RDF, $G(r)$, for Co–B glasses is interpreted as the superposition of the Co–Co and Co–B pair correlations. Shoulders which appeared near the 0.20 and 0.34 nm positions may be attributed to the Co–B correlations, because they become more pronounced for higher boron-containing alloy glasses. To demonstrate the contributions from different atomic pairs to total RDF, a more detailed analysis has been carried out by applying the concentration method [10, 19]. With the help of the anomalous scattering technique [10, 20], the partial RDFs to characterize a binary alloy were estimated. The detailed procedures are the same as those described previously [10, 19, 20] and thus are not duplicated here; only the essential features are given below for convenience of dissussion.

In a binary alloy, the total radial distribution function $G(r)$ may be expressed by the summation of the three partial radial distribution functions $G_{ij}(r)$, with a weighting factor w_{ij}, in the following form:

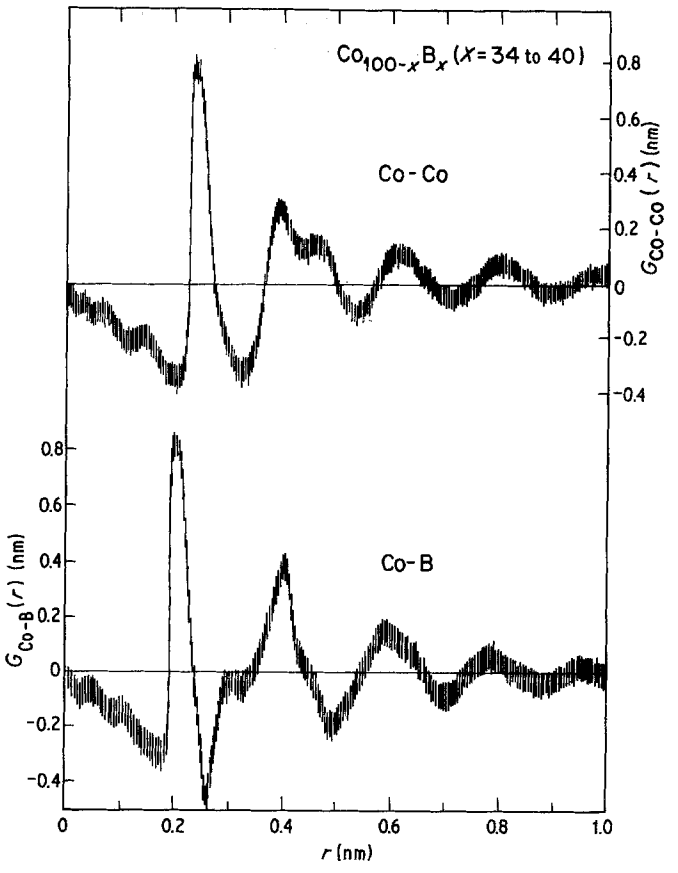

Figure 5 Partial functions $G_{ij}(r)$ for Co–Co and Co–B pairs of $Co_{100-x}B_x$ glasses (x = 34 to 40 at %).

$$G(r) = w_{11}G_{11}(r) + w_{22}G_{22}(r) + 2w_{12}G_{12}(r), \quad (2)$$

where

$$w_{ij} = c_i c_j f_i f_j / \langle f \rangle^2 \quad (3)$$

and

$$G_{ij}(r) = 4\pi r \rho_0 [\rho_{ij}(r)/(c_j\rho_0) - 1] = \frac{2}{\pi}\int_0^\infty Q[a_{ij}(Q) - 1] \sin(Qr)\, dQ, \quad (4)$$

where $a_{ij}(Q)$ is the so-called partial structure factor and the function $\rho_{ij}(r)$ means the distribution of type j atoms found at a radial distance of r from atom i at the origin. The partial functions $G_{ij}(r)$ could be estimated from Equation 2 by applying several methods [10]. The weighting factors for Co–Co, B–B and Co–B pairs in Equation 2 are as follows: 0.833, 0.008 and 0.159 for $Co_{66}B_{34}$ and 0.792, 0.012 and 0.196 for $Co_{60}B_{40}$, respectively. The weighting factor for B–B pairs to the total RDF is of the order of 0.01 for all samples of $Co_{100-x}B_x$ (x = 34 to 40) and so that the contribution of the B–B pairs to the total RDF is small. Therefore, in this work the B–B correlations are assumed to be random and only the partial RDF for Co–Co and Co–B pairs was estimated using the concentration method [19] with X-ray anomalous scattering technique [20]. The estimated partial functions $G_{ij}(r)$ for Co–Co and Co–B pairs in amorphous $Co_{100-x}B_x$ (x = 34 to 40) are illustrated in Fig. 5. The vertical lines in Fig. 5 denote the experimental uncertainty.

The basic profile of the partial functions is similar to the results for typical metal–metalloid glasses containing 15 to 25 at % metalloid. For example, a well-defined split in the second peak in total RDF characteristics for the structure of metal–metalloid glasses is found in the partial RDF of Co–Co pairs, although such a second peak is less distinct in the partial RDF of Co–B pairs, as shown in Fig. 5. The $G_{Co-B}(r)$ profile, meanwhile, shows a distinct split peak at smaller r (about 0.3 nm) of the second peak.

The distance r_{ij} and the co-ordination number n_{ij} of near neighbour correlations in the $Co_{60}B_{40}$ glass were estimated from the present $G_{ij}(r)$ by applying the same method of Sadoc and Dixmier [21] and are listed in Table II together with previous experimental data [7, 22]. The observed interatomic distance of unlike atom pairs is

TABLE II The near-neighbour correlations in amorphous metallic alloys of $Fe_{100-x}B_x$, calculated (calc) and experimentally determined (exp). In the calculations, the Fe–Fe distance is adjusted to the experimental one.

Compound A–B	Origin atom	A-element r(nm)	A-element n(atom)	B-element r(nm)	B-element n(atom)	Density (g cm^{-3})	Reference
Fe_5B_{15}	Fe	0.256	12.2	2.03	1.5	7.82	[7]
(cal)	B	0.20	7.7	–	–		
$Fe_{83}B_{17}$	Fe	0.256	10.7	2.27	1.6	7.41	[7]
(exp)	B	0.227	6.9	–	–		
$Fe_{75}B_{25}$	Fe	0.262	12.2	2.07	2.6	7.35	Present
(cal)	B	0.207	7.8	–	–		work
$Fe_{75}B_{25}$	Fe	0.260	10.5	2.27	2.4	7.22	[22]
(exp)	B	0.227	6.9	–	–		
$Fe_{60}B_{40}$	Fe	0.257	11.1	1.9	4.6	7.05	Present
(cal)	B	0.198	7.4	–	–		work
$Co_{60}B_{40}$	Co	0.257	10.2	2.03	3.9	7.48	Present
(exp)	B	0.20	6.2	–	–	(6.68)*	work

*The volume of density for $Fe_{60}B_{46}$ was estimated from the $Co_{60}B_{40}$ case.

considerably less than the value estimated from the Goldschmidt's radii; the interatomic distance of like atom pairs shows a slight expansion but agrees fairly well with the atomic diameter. This observation may be associated with the strong bonding between metal and metalloid atoms.

4.2. Model calculations and a comparison with experimental data

Fig. 4 illustrates a comparison of the calculated total RDF of $Fe_{85}B_{15}$, $Fe_{75}B_{25}$ and $Fe_{60}B_{40}$ with the experimental data; the experimental data of $Co_{60}B_{40}$ obtained in this work is given for comparison with the $Fe_{60}B_{40}$ case. In order to demonstrate the validity of the present model structure, Fig. 3 shows the calculated results of the $Fe_{100-x}P_x$ for $x = 15$, 20 and 25 at% [8] together with the experimental results recently obtained [15]. As shown in Fig. 3, the relaxed DRP model reproduces the experimental data fairly well, i.e., the sharp first-peak followed by the split in the second-peak and the height of the second sub-peak at larger r in the split second-peak region being lower than that of the first sub-peak.

As shown in Fig. 4, the total RDFs for boron contents of 15 and 25 at% agree well with the observed ones in their positions, peak heights and peak widths. In the case of $Fe_{60}B_{40}$, the overall agreement is reasonable except for the detailed peak profile. It may be worth mentioning that the shoulder due to the Fe–B contribution can be reproduced at the shorter distance side of the first-peak in the total RDF. However, the second-peak splitting in the model structure is much more clearly observed, although the first sub-peak becomes similarly narrow as in the experimental data. The model structure also indicates that the first sub-peak is enhanced with increasing boron content and the corresponding peak-height ratio of the glasses with higher boron content resembles rather closely that of the typical metal–metalloid glasses such as Fe–P alloys. Thus, these model calculations imply that the different peak profile of the second-peak for low boron-containing glasses is quite realistic and the present relaxed DRP model provides a good reproduction of the characteristic features observed in the compositional dependence of the structure for Fe–B glasses as well as the different peak profile for both Fe–B and Fe–P glasses.

In order to facilitate the understanding of this particular behaviour of boron-containing glasses, the partial RDF to characterize a binary alloy is also given in Figs 6, 7 and 8 with the available experimental data [7, 22] and the distances, r_{ij}, and co-ordination numbers, n_{ij}, of near neighbour correlations estimated from these partial RDFs are also listed in Table II. The structural features of the model calculations and experimental partial RDFs are summarized in the following:

(a) The basic profile of $G_{FeFe}(r)$ regarding the positions and relative amplitudes of the first and the second-peak are well reproduced by the relaxed DRP model, although there are differences in detail, e.g., the model yields more pronounced splitting in the second-peak than the experimental one. In the model, with increasing the boron content, x, in the first sub-peak (at smaller r) in the split second-peak region grows at the expense of the second sub-peak.

(b) Regarding the structural features of the

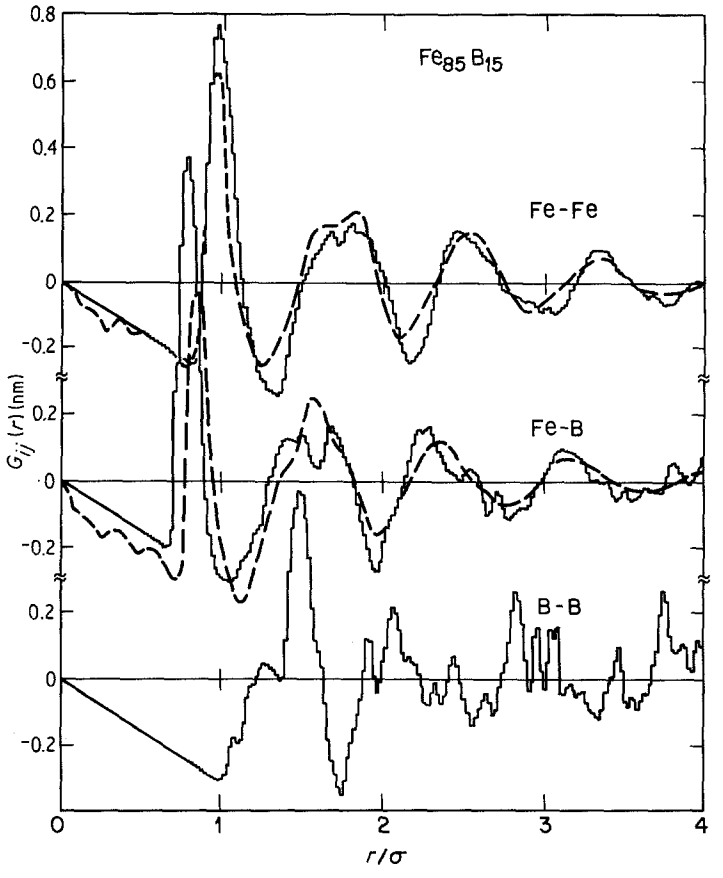

Figure 6 A comparison of model calculation with experimental data in the partial RDF for $Fe_{85}B_{15}$. Histogram: relaxed DRP model; broken curve: experimental data [7].

$G_{FeB}(r)$, the agreement between the results of the model and experimental data is acceptable. However, the split in the second-peak of the model for $Fe_{85}B_{15}$ is absent in the experimental one. The experimental $G_{FeB}(r)$ for $x = 40$ at% shows the shoulder in the second-peak region, while the shoulder at smaller r in the second-peak region is absent in the model structure of $G_{FeB}(r)$.

(c) As shown in Table II, the interatomic distances r_{FeFe} and r_{FeB} show a maximum and a plateau, respectively, for $x = 25$ and slightly decrease as x increases. The co-ordination number of Fe atom for boron in boron-containing glasses, $n_{BFe} = 7$, is smaller than that for phosphorus containing glasses, $n_{PFe} = 9$. The value of n_{FeFe} is of the order of 10 to 11 in the experimental data which is close to the typical close-packed structure of 12. The co-ordination numbers of near neighbour correlations in the model structure almost agree with the observed values. The calculated densities are slightly larger than those from the experimental data and this may account for the slightly larger values of the co-ordination numbers in the model.

(d) One of the distinct features of the present model calculations is the split first-peak for B–B pairs with three different compositions. Such behaviour was not observed in the unrelaxed DRP model structure. With increasing x, the first sub-peak (at smaller r) increases in amplitude at the expense of the second-peak in the first-peak region of $G_{BB}(r)$. The first sub-peak position, r_1, shifts to smaller r from $r_1 = 1.3\sigma$ for $x = 15$ to $r_1 = 1.1\sigma$ for $x = 40$, while the position of the second sub-peak, r_1, remains the same value of $r_1' = 1.4\sigma$ for three composition. This particular structural feature of B–B pairs may account for part of the characteristic behaviour for the boron-containing glasses. However, no definite conclusion for the split first-peak of the partial RDF of B–B pairs could be drawn from the presently available information. The experimental data for the B–B partial RDF would be strongly desirable.

(e) The basic peak profile of the partial RDF for the Fe–Fe pairs is very close to the total RDF of the X-ray data and the first sub-peak in the second-peak region of the total RDF should be interpreted as the superposition of the correlation

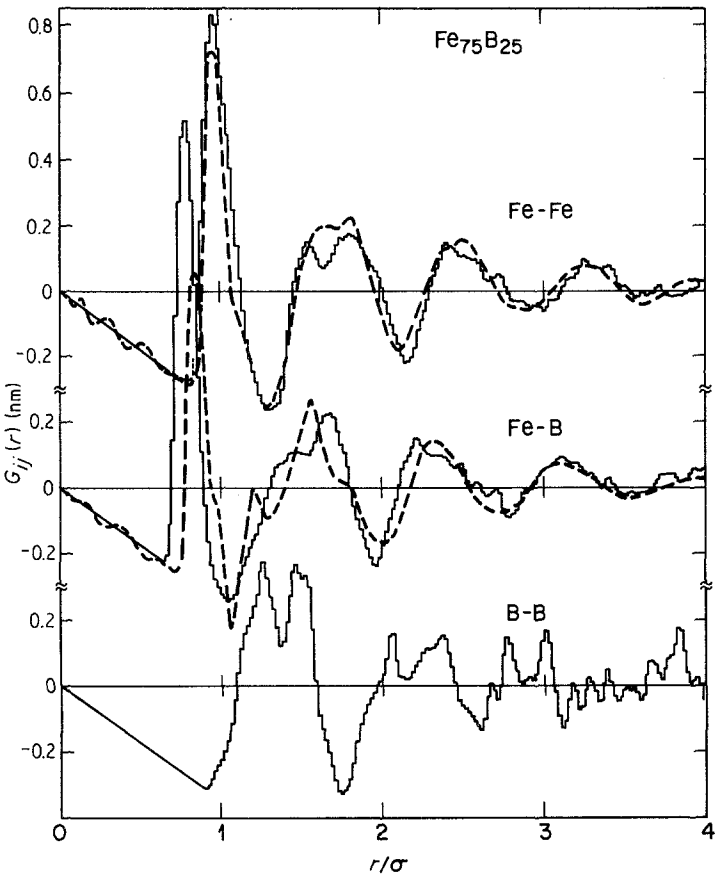

Figure 7 A comparison of model calculation with experimental data in the partial RDF for $Fe_{75}B_{25}$. Histogram: relaxed DRP model; broken curve; experimental data [22].

of the Fe–Fe and Fe–B pairs. It is also evident that the correlation of the Fe–B pairs contributes to the shoulder at the smaller-r side of the first-peak in the total RDF for $Fe_{60}B_{40}$.

As shown in Figs 6 to 8, the structural features of respective pairs are well produced by the present relaxed DRP model, although the origin of the observed difference from the experimental data cannot be certainly identified at the present time. However, the present results may indicate that the partial distribution functions for unlike atom pairs of Fe–B are rather sensitive to the potential functions employed in the model calculation, whereas, the distribution function of the major constituents, Fe–Fe pairs, is determined mainly by the geometrical DRP structure. The decrease in both atomic distances r_{ij} and co-ordination numbers n_{ij} for the Fe–Fe and Fe–B pairs for $x \geqslant 25$ (see Table II) also seems to suggest the appreciable compositional dependence of the structure of boron-containing glasses. The influence of composition on the structure in amorphous Fe–B alloys is further clearly observed in the model partial structure of the B–B pairs, as stated previously.

Based on the previous experimental results for various metallic glasses of metal–metalloid type [10, 15], any metalloid atoms could not be in hard contact with other metalloid atoms. However, for the higher boron content glasses, it is conceivable that some of the boron atoms may be in hard contact and thus the short-range ordering in these glassy structures may prevail over those expected in the corresponding crystalline phases. It may be noted that the shortest distance of the B–B pairs becomes as short as 0.7σ, being comparable with the atomic diameter of boron atoms of 0.58σ in the model structure of $Fe_{60}B_{40}$ after the relaxation process, as shown in Fig. 8, although the position of the split first peak of $G_{BB}(r)$ still remains larger than 1.0σ. The present model calculation suggests that the major number of boron atoms are still in isolation, which is consistent with the Goldschmidt suggestion that the boron atoms are prohibited themselves from direct contact for lower borides such as M_2B (M = Fe, Co or Ni) [23]. A proportion

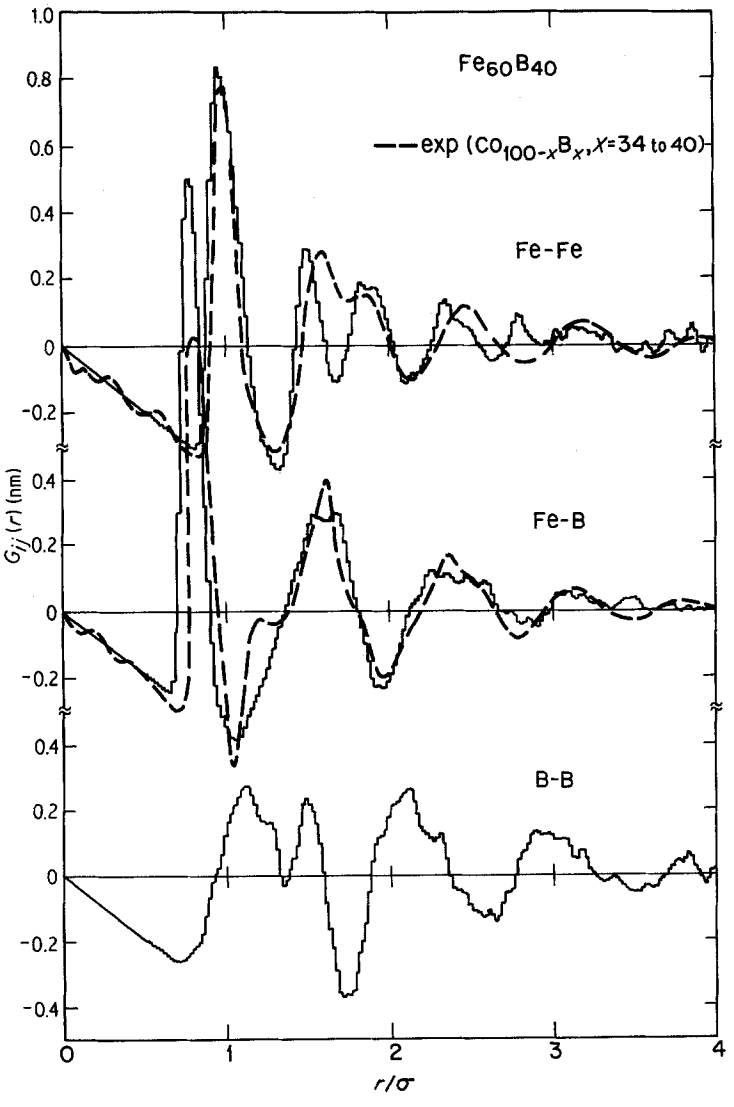

Figure 8 A comparison of model calculation with experimental data in the partial RDF for $Fe_{60}B_{40}$. Histogram: relaxed DRP model; broken curve: experimental data of $Co_{100-x}B_x$ glasses ($x = 34$ to 40) obtained in this work.

of the metalloids pairs may be in hard contact, which is more feasible in the higher boron-containing glasses, but even so the number of such metalloid pairs is not large, although a quantitive discussion is not possible at the present time. Further experimentation, particularly to determine the partial RDF of the B–B pairs, is desirable to quantitatively clarify these points.

Acknowledgements

One of the authors (YW) expresses thanks to the Ito Science Foundation and the RCA Research Laboratories (Japan) for the provisions of grants in 1979–80.

References

1. Proceedings of the 4th International Conference on Liquid and Amorphous Metals (LAM4), Grenoble, 1980, *J. de Physique Colloque*, No. C8, **41** (1980).
2. R. HASEGAWA and R. RAY, *J. Appl. Phys.* **49** (1978) 4175.
3. F. E. LUBORSKY and H. H. LIBERMANN, *Appl. Phys. Lett.* **33** (1978) 233.
4. H. HIROYOSHI, K. FUKAMACHI, M. KIKUCHI, A. HOSHI and T. MASUMOTO, *Phys. Lett.* **65A** (1978) 163.
5. Y. WASEDA and H. S. CHEN, *Phys. Stat. Sol. (a)* **49** (1978) 387.
6. N. COWLAM, M. SAKATA and H. A. DAVIES, *J. Phys. F.* **9** (1979) L203.
7. T. FUJIWARA, H. S. CHEN and Y. WASEDA, *ibid.* **11** (1981) 1327.
8. T. FUJIWARA and Y. ISHII, *ibid.* **10** (1980) 1901.
9. A. INOUE, A. KITAMURA and T. MASUMOTO, *Trans. Japan. Inst. Met.* **20** (1979) 404.
10. Y. WASEDA, "The Structure of Non-Crystalline Materials" (McGraw-Hill Book Co., New York, 1980) p. 87.
11. K. FURUKAWA, *Rep. Progr. Phys.* **25** (1962) 392.

12. A. RAHMAN, *J. Chem. Phys.* **42** (1965) 3540.
13. A. J. GREENFIELD, J. WELLENDORF and N. WISER, *Phys. Rev.* **A4** (1971) 1607.
14. R. KAPLOW, S. L. STRONG and B. L. AVERBACH *ibid.* **138** (1965) A1336.
15. Y. WASEDA, *Prog. Mater. Sci.* **26** (1981) 1.
16. T. EGAMI, *J. Mater. Sci.* **13** (1978) 2587.
17. A. WILLIAMS and W. L. JOHNSON, *J. Non-Cryst. Solids* **34** (1979) 121.
18. E. NOLD, S. STEEB and P. LAMPARTER, *Z. Naturforsch.* **35a** (1980).
19. N. C. HALDER and C. N. J. WAGNER, *J. Chem. Phys.* **43** (1967) 4385.
20. Y. WASEDA and S. TAMAKI, *Phil. Mag.* **32** (1975) 951.
21. J. F. SADOC and J. DIXMIER, *Mater. Sci. Eng.* **23** (1976) 187.
22. Y. WASEDA, Proceedings of the 3rd International Conference on Rapidly Quenched Metals, Brighton, July 1978 (The Metals Society, London, 1978) p. 352.
23. H. J. GOLDSCHMIDT, "Interstitial Alloys" (Plenum Press, New York, 1967) p. 254.

Received 1 September
and accepted 28 September 1981